



# Probing conformational transitions towards mutagenic Watson–Crick-like G·T mismatches using off-resonance sugar carbon $R_{1\rho}$ relaxation dispersion

Atul Rangadurai<sup>1</sup> · Eric S. Szymanski<sup>1,2</sup> · Isaac Kimsey<sup>1,2</sup> · Honglue Shi<sup>3</sup> · Hashim M. Al-Hashimi<sup>1,3</sup> 

Received: 14 March 2020 / Accepted: 13 July 2020 / Published online: 12 August 2020  
© The Author(s) 2020

## Abstract

NMR off-resonance  $R_{1\rho}$  relaxation dispersion measurements on base carbon and nitrogen nuclei have revealed that wobble G·T/U mismatches in DNA and RNA duplexes exist in dynamic equilibrium with short-lived, low-abundance, and mutagenic Watson–Crick-like conformations. As Watson–Crick-like G·T mismatches have base pairing geometries similar to Watson–Crick base pairs, we hypothesized that they would mimic Watson–Crick base pairs with respect to the sugar-backbone conformation as well. Using off-resonance  $R_{1\rho}$  measurements targeting the sugar C3' and C4' nuclei, a structure survey, and molecular dynamics simulations, we show that wobble G·T mismatches adopt sugar-backbone conformations that deviate from the canonical Watson–Crick conformation and that transitions toward tautomeric and anionic Watson–Crick-like G·T mismatches restore the canonical Watson–Crick sugar-backbone. These measurements also reveal kinetic isotope effects for tautomerization in D<sub>2</sub>O versus H<sub>2</sub>O, which provide experimental evidence in support of a transition state involving proton transfer. The results provide additional evidence in support of mutagenic Watson–Crick-like G·T mismatches, help rule out alternative inverted wobble conformations in the case of anionic G·T<sup>-</sup>, and also establish sugar carbons as new non-exchangeable probes of this exchange process.

**Keywords** Tautomers · Anions · Replication error · Nucleic acid dynamics · Chemical exchange · Sugar pucker

## Introduction

In their paper describing the structure of the DNA double helix, James Watson and Francis Crick proposed that spontaneous mutations could arise when nucleotide bases adopt rare and energetically less favorable tautomeric forms as this could allow wobble mismatches such as A·C and G·T to adopt a geometry similar to that of canonical G·C

and A·T Watson–Crick (WC) base pairs (bps) (Watson and Crick 1953). Two decades later, Topal and Fresco extended this idea, and proposed that the probability with which rare tautomers form could determine the probability of misincorporating mismatches during replication and translation (Topal and Fresco 1976; Topal and Fresco 1976). During the same period, it was shown that WC-like G·T mismatches could also form via ionization of the thymine base Lawley and Brookes 1962; Sowers et al. 1987; Lawley and Brookes 1961. This anionic WC-like species could explain the increase in G·T misincorporation probability with increasing pH. Yu et al. (1993) Together, the tautomeric and anionic WC-like G·T mismatches could rationalize why chemical modifications that stabilize or mimic either tautomeric (Harris et al. 2003; Budowsky 1976; Woodside and Guengerich 2002; Cantara et al. 2013; Vendeix et al. 2012; Kurata et al. 2008; Ikeuchi et al. 2010) or ionic (Yu et al. 1993; Strebiter et al. 2018; Weixlbaumer et al. 2007) forms of the bases increase the probability of errors during replication and translation.

**Electronic supplementary material** The online version of this article (<https://doi.org/10.1007/s10858-020-00337-7>) contains supplementary material, which is available to authorized users.

✉ Hashim M. Al-Hashimi  
hashim.al.hashimi@duke.edu

<sup>1</sup> Department of Biochemistry, Duke University School of Medicine, Durham, NC 27710, USA

<sup>2</sup> Present Address: Nymirum, 4324 S. Alston Avenue, Durham, NC 27713, USA

<sup>3</sup> Department of Chemistry, Duke University, Durham, NC 27710, USA

Studies over the past decade have provided additional structural and kinetic evidence in support of WC-like mismatches having important roles in the generation of errors during replication and translation. WC-like mismatches have been observed in crystal structures of DNA polymerases (Wang et al. 2011; Bebenek et al. 2011; Koag et al. 2014; Koag and Lee 2018; Sharma et al. 2013) and the ribosome (Rozov et al. 2018; Rozov et al. 2016; Rozov et al. 2015; Demeshkina et al. 2012) in catalytically active conformations. Spontaneous transitions between wobble G·T/U mismatches and short-lived, low-abundance WC-like tautomeric and anionic G·T/U mismatches have also been observed in solution using off-resonance  $R_{1\rho}$  NMR relaxation dispersion (RD) experiments (Rangadurai et al. 2019; Palmer and Massi 2006) in both DNA and RNA duplexes (Fig. 1a). Szymanski et al. (2017), Kimsey et al. (2018) and Kimsey et al. (2015) WC-like G·T mismatches were shown to form with probabilities that could quantitatively explain the ~1000 fold reduction in misincorporation rate for G·T mismatches

compared to G·C bps (Kimsey et al. 2018). Beyond their roles in the generation of errors during replication and translation, WC-like mismatches have also been proposed to play roles in the generation of errors during transcription (Phillips and Brown 1967; Singer and Spengler 1981; Li et al. 2014) and in DNA damage repair (Freudenthal et al. 2015).

Dynamic transitions between wobble and WC-like G·T/U mismatches (Fig. 1a) (Szymanski et al. 2017; Kimsey et al. 2018; Kimsey et al. 2015) have so far been studied by measuring off-resonance  $R_{1\rho}$  NMR RD data for nitrogen and carbon spins in the nucleotide bases. These include the imino nitrogens (G·N1 and T/U·N3), which experience large downfield shifts (~50 ppm) upon deprotonation, as well as the aromatic carbons (G·C8 and T·C6) and amino nitrogen (G·N2) atoms, which experience smaller downfield shifts (~2–4 ppm). These RD measurements (Kimsey et al. 2018; Kimsey et al. 2015) combined with single atom substitution experiments have identified three distinct WC-like G·T/U mismatches stabilized by WC-like hydrogen-bonds

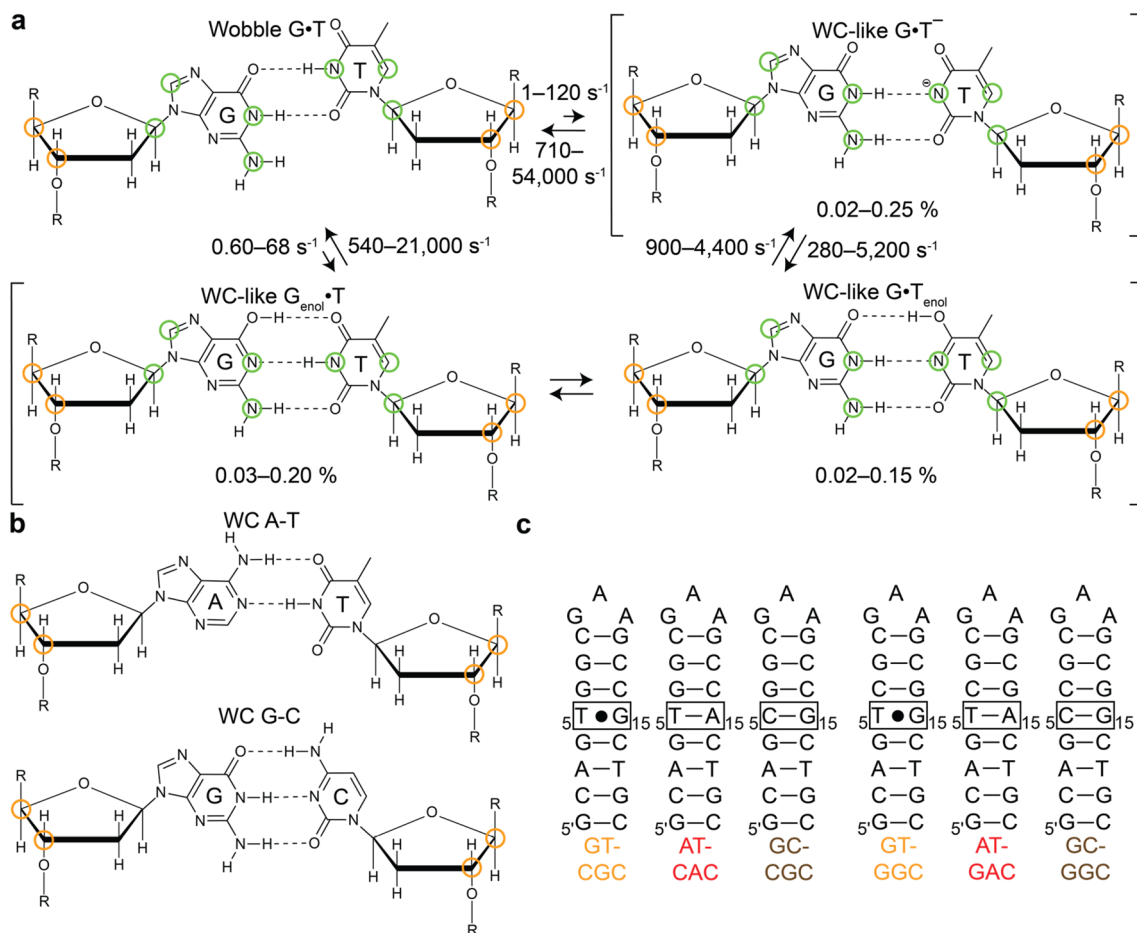


**Fig. 1** a Exchange between wobble and, tautomeric and anionic WC-like G·T mismatches<sup>29</sup>. Green circles denote RD probes used to characterize the exchange in previous studies (Szymanski et al. 2017; Kimsey et al. 2015). b A-T and G-C Watson-Crick bps in DNA.

Orange circles denote RD probes used to characterize formation of WC-like mismatches in this study. c DNA constructs used in this study

(Szymanski et al. 2017). These include two rapidly interconverting tautomeric forms in which either the G or T/U base can tautomerize ( $G^{\text{enol}}$  and  $T^{\text{enol}}/U^{\text{enol}}$ ) to form tautomeric WC-like  $G^{\text{enol}}\cdot T/U$  and  $G\cdot T^{\text{enol}}/U^{\text{enol}}$  mismatches, and an anionic species in which the T/U ionizes to form anionic WC-like  $G\cdot T^-/U^-$  mismatches. However, it remains unknown whether these transitions are also accompanied by changes in the sugar-backbone conformation.

Compared to WC bps, G·T wobble mismatches adopt non-canonical sugar-backbone conformations (Allawi and SantaLucia 1998; Patel et al. 1982; Hare et al. 1986; Hunter et al. 1987). If the transient low-abundance species measured by NMR RD does indeed represent a WC-like G·T mismatch, one would expect that such a transition might restore a canonical WC-like sugar-backbone conformation (Fig. 1b). In principle, one can probe such transient conformational changes in the sugar-backbone using RD measurements targeting the sugar carbons C3' and C4' (Shi et al. 2018; Clay et al. 2017). Beyond confirming the identity of the transient low-abundance species measured previously by RD and establishing sugar RD as a new probe of this exchange process, determining the sugar-backbone conformation of Watson–Crick like G·T mismatches is important for assessing their mutagenicity as it defines the placement of the phosphate oxygen atom, which is integral for polymerization chemistry during replication.

Here, we used off-resonance sugar carbon  $R_{1\rho}$  measurements, a structure survey, and computational Molecular Dynamics (MD) simulations to characterize changes in the sugar-backbone accompanying the formation of tautomeric and anionic WC-like G·T mismatches. The results show that the G·T wobble mismatch adopts a non WC-like sugar-backbone conformation and that transitions toward either tautomeric or anionic WC-like G·T mismatches restore the canonical WC-like sugar-backbone conformation. These measurements extend the definition of a WC-like bp to encompass the sugar and backbone, help rule out alternative inverted wobble conformations in the case of anionic  $G\cdot T^-$ , and also offer new non-exchangeable probes of this exchange process that can enable measurements over a broad range of structural environments.

## Materials and methods

### Crystal structure survey of G·T mismatches

All crystal structures containing DNA with resolution better than 3 Å as of April 27th 2017 were downloaded from the Protein Data Bank (PDB) (Berman et al. 2000). Structures were analyzed using an in-house Python script to identify wobble G·T mismatches that are flanked by two WC bps on either side to mimic a duplex like environment. A total of

15 G·T mismatches belonging to 14 distinct structures were identified out of a total of 5906 deposited structures in the PDB containing nucleic acids (Supplementary Table S1). The torsion angles and C1'–C1' distance of the mismatched bps were computed and compared with a set of unmodified G·C and A·T Watson–Crick bps from free (not bound to proteins/ligands) DNA structures placed in a similar structural context with B form helical geometry as determined using DSSR (Lu et al. 2015). The BI/BII phosphate conformation was determined by first converting the  $\epsilon$  and  $\zeta$  torsion angles to the  $[0^\circ, 360^\circ]$  range, taking the difference  $\epsilon - \zeta$ , and then converting the resultant angle into the  $[0^\circ, 360^\circ]$  range (see Figs. 2a and 3). A given phosphate was classified as BII if this difference was in the range  $[20^\circ, 200^\circ]$ , otherwise it was classified as BI.

To define the movements of the G and T bases required to form a wobble G·T mismatch when starting from a WC bp (Fig. 2b), the coordinates for the G·T mismatches along with one WC bp on either side of the mismatch were extracted from the above crystal structures. An idealized triplet of bps with a G·C bp in the middle was constructed using 3DNA (Lu and Olson 2003). Triplets of G·T mismatches were superimposed on the idealized triplet of bps using the sugar atoms of the bps neighboring the mismatch and the idealized G·C bp. An overlay of the G·T mismatches with the idealized G·C bp after superposition is shown in Fig. 2b.

### MD simulations

All MD simulations were performed using the ff99 AMBER force field (Cheatham et al. 1999) with bsc0 corrections for DNA (Perez et al. 2007), using periodic boundary conditions as implemented in the AMBER MD simulation package (Salomon-Ferrer et al. 2013). DNA duplexes with G·T or G·C/A·T WC bps used in the MD simulations (Supplementary Figure S2) were derived from the hairpins (GT-CGC/GT-GGC/AT-CAC/AT-GAC/GC-CGC/GC-GGC) used for the NMR measurements (Supplementary Figure S4) by elongating by two G·C/A·T bps on either end. Starting structures of the WC base paired helices for the simulations were generated by creating idealized B-DNA helices using 3-DNA (Lu and Olson 2003). Corresponding starting structures containing G·T mismatches were obtained by mutating the WC base paired structures. Starting structures were solvated using a truncated octahedral box of SPC/E (Berendsen et al. 1987) water molecules with box size chosen such that the boundary was at least 10 Å away from the DNA atoms.  $\text{Na}^+$  ions treated using the Joung–Cheatham ion parameters (Joung and Cheatham 2008) were then added to neutralize the charge of the system. Minimization, equilibration and production runs (500 ns) were then performed as described previously (Rangadurai et al. 2018). A set of evenly (5 ps)

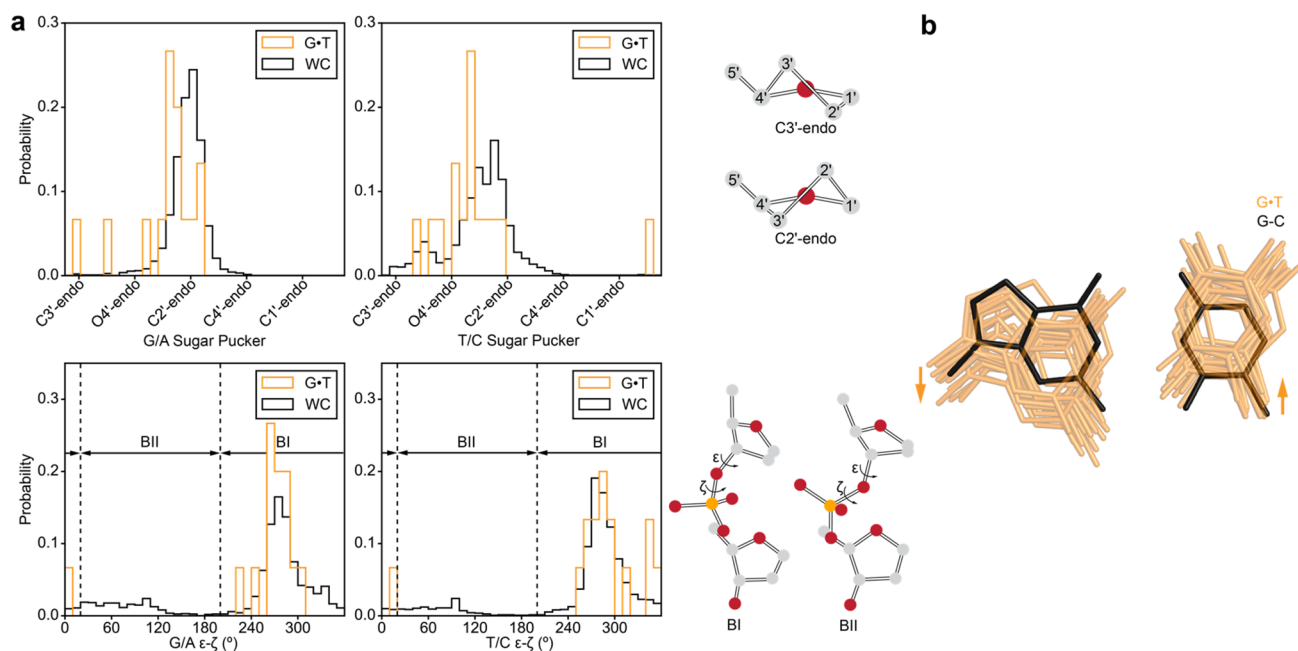


**Fig. 2** **a** Histograms comparing the sugar pucker and  $\epsilon$ - $\zeta$  torsion angle for G-T mismatches (orange) and WC bps (black), as obtained from a survey of crystal structures in the PDB<sup>41</sup> (Materials and Methods). The angles for G and T in the G-T mismatch were compared to those of G/A and T/C in the WC bps, respectively. The C2'-endo and C3'-endo sugar pucker conformations as well as BI and BII backbone conformations

are shown on the right. **b** Overlay of crystal structures of G-T mismatches obtained from a survey of the PDB (orange) and an idealized G-C bp (black) (Materials and Methods). Arrows indicate direction of movement of bases required for transition from a WC to a wobble bp conformation

spaced snapshots was used for subsequent analysis using the CPPTRAJ (Roe and Cheatham 2013) suite of programs.

## Sample preparation

### Unlabeled DNA oligonucleotides

All unlabeled and unmodified DNA oligonucleotides (GT-CGC, GT-GGC, AT-CAC, AT-GAC, GC-CGC and GC-GGC, see Fig. 1c, Supplementary Figure S4) were purchased from Integrated DNA Technologies with standard desalting purification. Unlabeled DNA oligonucleotides containing *N*<sup>1</sup>-methyl deoxy Guanosine (m<sup>1</sup>G, GT-CGC<sup>m<sup>1</sup>G</sup>) or deoxyisoGuanosine (isoG, GT-CGC<sup>isoG</sup> and GT-GGC<sup>isoG</sup>) (Supplementary Figure S4) were synthesized in-house using a MerMade 6 oligo synthesizer. In particular, standard (bz-A, ac-C, n-ibu-G and T) and modified DNA phosphoramidites (n,n-dmf-m<sup>1</sup>G, Chemgenes and dmf-isoG, Glen Research) were used with a coupling time of 1 min, with the final 5'-DMT group being retained during synthesis. The oligonucleotides were then cleaved from the supports (1  $\mu$ mol, 1000 Å) using ~1 mL of AMA (1:1 ratio of ammonium hydroxide and methylamine) for 30 min and deprotected at room temperature for 2 h. The oligonucleotides were then purified using Glen-Pak DNA cartridges followed by ethanol precipitation.

### Site-labeled DNA oligonucleotides

Site labeled DNA oligonucleotides (sIGT-CGC and sIGT-GGC) uniformly <sup>13</sup>C, <sup>15</sup>N labeled at positions T5 and G15 (Supplementary Figure S4), were purchased from the Yale Keck Oligonucleotide Synthesis Facility with cartridge purification.

### Fully labeled DNA oligonucleotides

Uniformly <sup>13</sup>C/<sup>15</sup>N isotopically labeled fIGT-CGC (Supplementary Figure S4) was biochemically synthesized using the Zimmer and Crothers method (Zimmer and Crothers 1995). A chemically synthesized DNA hairpin template containing a 3' ribonucleotide (IDT) was used in addition to Klenow fragment DNA polymerase (New England Biolabs) and <sup>13</sup>C/<sup>15</sup>N isotopically labeled deoxy nucleoside triphosphates (Silantes). The reaction mixture was centrifuged to remove pyrophosphate and then incubated with NaOH (final concentration 0.3 M) for 3 h at 55 °C for cleavage of the target oligonucleotide from the template. The mixture was then concentrated to 1.5 mL using a 3 kDa molecular weight cutoff centrifugal concentrator (Millipore Sigma). This was followed by addition of 1.5 mL of a formamide based denaturing loading dye. The mixture was then heated at 95 °C for 5 min for denaturation, and then loaded onto a denaturing gel

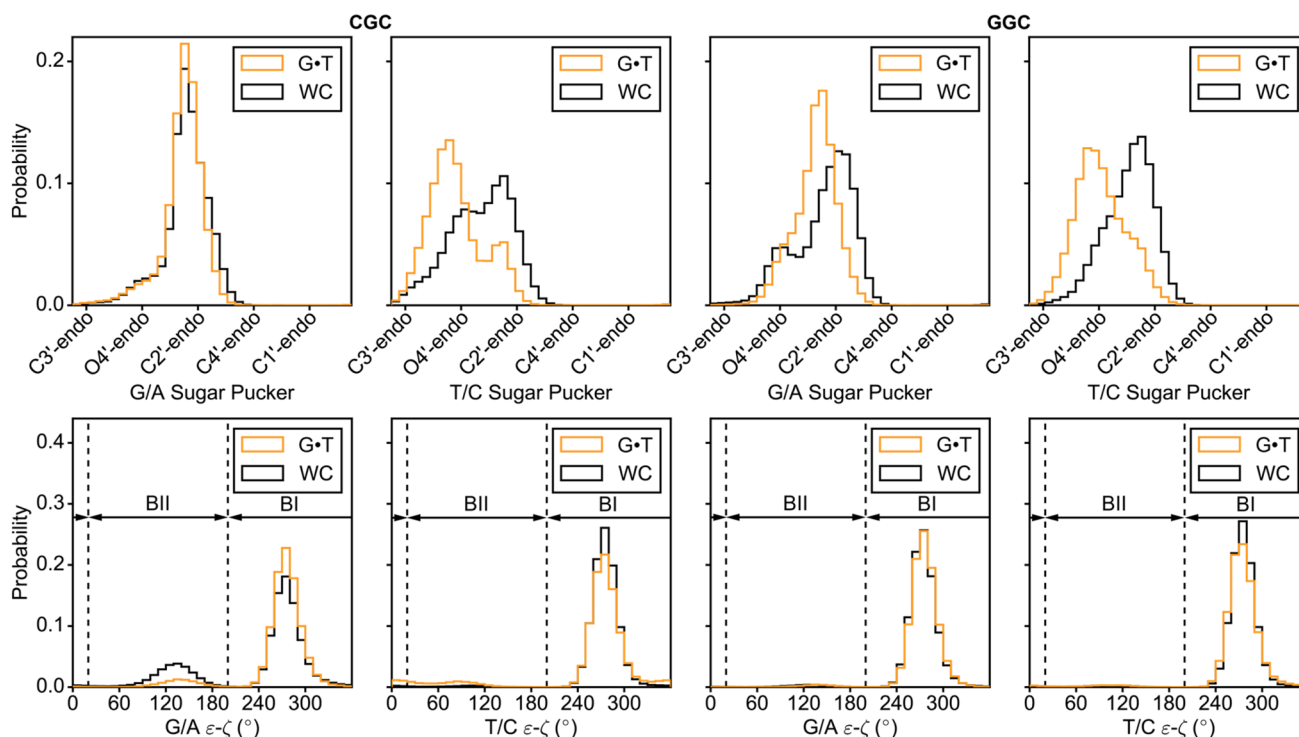


**Fig. 3** Histograms comparing the sugar pucker and  $\varepsilon$ - $\zeta$  torsion angle for G-T mismatches (orange) and WC bps (black), as obtained from MD simulations on DNA duplexes in two different sequence contexts (CGC and GGC, Supplementary Figs. S2, S3, Materials and Methods). The sugar pucker and torsion angles of the G and T in the

G-T mismatch were compared to those of G/A and T/C in WC bps, respectively. The puckers and torsion angles for the WC bps were obtained by averaging over individual simulations with G-C and A-T bps in place of G-T

(20% polyacrylamide/8 M urea) for separation of the target oligonucleotide from other nucleic acid species. Gel bands corresponding to the target single strands were identified by UV-shadowing and subjected to electroelution (Whatman, GE Healthcare) followed by ethanol precipitation.

### Sample annealing and buffer exchange

Oligonucleotides (following ethanol precipitation or as purchased) were re-suspended in water. The samples were annealed by heating at  $T = 95$  °C for ~5 min followed by cooling on ice for ~1 h. Following annealing, the samples were exchanged three times into the desired buffer using centrifugal concentrators (4 mL, Millipore Sigma) with a 3 kDa molecular weight cutoff. 10% by volume of  $D_2O$  was added to the samples prior to the NMR experiments for establishing C1'-H1' and C8-H8 assignments (see below). Samples were then lyophilized once and re-suspended in  $D_2O$  for establishing C3'-H3' and C4'-H4' assignments (see below) and performing RD measurements unless mentioned otherwise.

### NMR buffer

Sodium phosphate buffer for NMR measurements was prepared by the addition of equimolar solutions of sodium phosphate monobasic and dibasic salts, sodium chloride, and EDTA to give final concentrations (unless mentioned otherwise) of 15 mM (phosphate), 25 mM and 0.1 mM respectively. The pH was then adjusted by the addition of phosphoric acid or sodium hydroxide, after which the buffers were brought up to the desired volume and filtered and stored for further usage.

### NMR spectroscopy

All NMR experiments were performed on a 700 MHz Bruker Avance 3 spectrometer equipped with a triple-resonance HCN cryogenic probe. All experiments were performed at pH 6.9 and at  $T = 25$  °C in NMR buffer unless stated otherwise. The NMR data was processed and analyzed using NMRpipe (Delaglio et al. 1995) and Goddard and Kneller (2008)

## Resonance assignments

The sugar C1'-H1' and base C6-H6/C2-H2/C8-H8 resonances were assigned using 2D [<sup>1</sup>H, <sup>1</sup>H] Nuclear Overhauser Effect Spectroscopy (NOESY) and 2D [<sup>13</sup>C, <sup>1</sup>H] Heteronuclear Single Quantum Coherence (HSQC) spectra of samples in 90% H<sub>2</sub>O/10% D<sub>2</sub>O. The C3'-H3' and C4'-H4' resonances were assigned using 2D [<sup>1</sup>H, <sup>1</sup>H] Total Correlation Spectroscopy (TOCSY) and 2D [<sup>13</sup>C, <sup>1</sup>H] HSQC spectra of samples in 100% D<sub>2</sub>O. Spectra of GT-CGC<sup>m1G6</sup> were collected at pH 5.0, 25 °C in order to promote formation of the m<sup>1</sup>G6-C14<sup>+</sup> Hoogsteen bp, while those of GT-CGC<sup>isoG</sup> and GT-GGC<sup>isoG</sup> were collected at a lower temperature (pH 6.9, 10 °C) to minimize alternative tautomeric forms of isoG, which are known to be populated at higher temperatures<sup>54</sup>.

## Off-resonance <sup>13</sup>C/<sup>15</sup>N R<sub>1ρ</sub> RD measurements

Off-resonance <sup>13</sup>C/<sup>15</sup>N R<sub>1ρ</sub> measurements were performed using 1D R<sub>1ρ</sub> schemes employing selective Hartman-Hahn magnetization transfers as described previously (Hansen et al. 2009; Korzhnev et al. 2005; Nikolova et al. 2012). Weak matched <sup>1</sup>H and <sup>13</sup>C/<sup>15</sup>N RF fields were used to transfer magnetization selectively from protons to the <sup>13</sup>C/<sup>15</sup>N nucleus of interest. The longitudinal <sup>13</sup>C/<sup>15</sup>N magnetization thus produced was allowed to relax for 5 ms to allow equilibration of ground state and excited state populations and then tilted along the appropriate effective field direction. Then a <sup>13</sup>C/<sup>15</sup>N spin-lock was applied for a maximal duration (< 120 ms for <sup>15</sup>N and < 60 ms for <sup>13</sup>C) chosen so as to achieve ~ 70% loss in signal intensity at the end of the relaxation period. The signal intensity was recorded for 3–10 delays equally spaced over the relaxation period. Spin-lock powers and offsets used are given in Supplementary Table S2. The RD measurements were performed on lyophilized samples in D<sub>2</sub>O at pH 6.9 and T = 25 °C in NMR buffer unless stated otherwise. Use of D<sub>2</sub>O is especially important for C3'/C4' RD measurements in order to avoid interference from the water signal; for this reason, the C3' and C4' RD measurements were performed in D<sub>2</sub>O unless stated otherwise.

## Fitting of R<sub>1ρ</sub> RD data

R<sub>1ρ</sub> values for a given spin-lock power and offset were obtained by extracting the peak intensities as a function of delay time using NMRPipe (Delaglio et al. 1995) and then fitting them to a mono-exponential function (Kimsey et al. 2015). Errors in R<sub>1ρ</sub> (σ<sub>R1ρ</sub>) were estimated using a Monte-Carlo scheme as described previously (Rangadurai et al. 2019). Numerical integration of the Bloch–McConnell (B-M) equations were used to fit R<sub>1ρ</sub> values as a function of spin-lock power and offset to 2-state or 3-state exchange

models, by minimizing  $\chi^2 = \sum \frac{R_{1\rho,meas} - R_{1\rho,calc}}{R_{1\rho}}$ , using least squares minimization as described previously (Rangadurai et al. 2019). R<sub>1ρ,meas</sub> and R<sub>1ρ,calc</sub> are the measured and calculated R<sub>1ρ</sub> values, respectively, and the summation is over all spin-lock power offset combinations. The fitted exchange parameters for the 2-state individual fits were p<sub>B</sub>, k<sub>exAB</sub>, R<sub>1</sub>, R<sub>2</sub> and Δω, while those for the 3-state individual fits were p<sub>B</sub>, p<sub>C</sub>, k<sub>exAB</sub>, k<sub>exAC</sub>, R<sub>1</sub>, R<sub>2</sub>, Δω<sub>AB</sub> and Δω<sub>AC</sub>. Global fits were performed by sharing p<sub>B</sub>/p<sub>C</sub> and k<sub>exAB</sub>/k<sub>exAC</sub> across multiple nuclei.

It has been shown that base carbon and imino nitrogen RD measurements on G-T mismatches can passively sense the WC to Hoogsteen exchange of neighboring bps (Kimsey et al. 2015), a phenomenon that will hereafter be referred to as “Hoogsteen blowback”, in addition to the exchange of the mismatch itself into a WC-like species. In principle, G-T mismatches in GT-CGC and GT-GGC (Fig. 1c, Supplementary Figure S4) can experience Hoogsteen blowback due to both of the neighboring G-C bps, thereby introducing extraneous contributions to the measured RD data. The Hoogsteen blowback contribution from the G6-C14 bp is expected to be significant for T5-C3' in the G-T mismatch in GT-CGC. This is because formation of Hoogsteen bps is accompanied by sizeable (~ 2 ppm) downfield shifts in the C3' carbon of the nucleotide 5' to the purine (Shi et al. 2018). Hoogsteen blowback contributions are expected to be smaller for GT-GGC since none of the mismatched nucleotides are 5' to the purines of the neighboring WC bps. The WC to Hoogsteen exchange at the G6-C14 bp was quantified by measuring <sup>13</sup>C R<sub>1ρ</sub> RD on G6-C1' in fGT-CGC (Supplementary Figs. S4 and S6). The G6-C1' RD data could be directly fit to the Bloch–McConnell equations assuming a two-state exchange process to characterize the WC to Hoogsteen exchange at the G6-C14 bp. It should be noted that G6-C1' is not expected to passively sense the transition between wobble and WC-like G-T as Δω<sub>G6-C1'</sub>, estimated as the difference in chemical shifts of G6-C1' between GT-CGC and, GC-CGC or AT-CAC is < ~ 0.3 ppm (Supplementary Figure S5).

Including a shared Hoogsteen blowback exchange process when individually fitting <sup>13</sup>C/<sup>15</sup>N R<sub>1ρ</sub> RD profiles of the G-T mismatch in slGT-CGC to a 3-state exchange model in a star-like (Trott and Palmer 2004) topology resulted in exchange parameters for the wobble to WC-like exchange that are more similar across different nuclei relative to parameters obtained from 2-state fits which do not account for Hoogsteen blowback (Supplementary Tables S3 and S4, Supplementary Figure S7). Moreover, the <sup>13</sup>C and <sup>15</sup>N R<sub>1ρ</sub> RD data for multiple nuclei of the G-T mismatch could also be globally fitted to a 3-state exchange model sharing p<sub>B</sub> and k<sub>ex</sub> for the exchange to a WC-like species with the inclusion of a shared Hoogsteen blowback exchange contribution in

a star-like (Trott and Palmer 2004) topology (Supplementary Tables S3 and S4, Fig. 5a, Supplementary Figure S9a). In addition, the populations of the WC-like G·T mismatch obtained from RD measurements in 90% H<sub>2</sub>O:10% D<sub>2</sub>O (Supplementary Table S3) and 100% D<sub>2</sub>O (Supplementary Table S4) were in better agreement with each other when globally fitting the data with the inclusion of a shared Hoogsteen blowback exchange process, relative to when blowback was not considered during fitting (Supplementary Figure S8a). Reasonable estimates of  $\Delta\omega$  for the atoms of the G·T mismatch on the formation of a G6-C14 Hoogsteen bp were also obtained from shared fitting of the RD data, that were similar to the difference in chemical shifts of the atoms between GT-CGC<sup>m1G6</sup> and GT-CGC (Supplementary Tables S3 and S4, Supplementary Figure S8b). The poor agreement seen for T5-C6 is likely due to *N*<sup>1</sup>-methylation of G6 in GT-CGC<sup>m1G6</sup>. RD profiles for s1GT-CGC obtained from a global fit with the inclusion of a shared blowback exchange are displayed in Fig. 5a and Supplementary Figs. 6 and 9a. Fits to RD profiles for s1GT-GGC to a 2-state exchange model without inclusion of a shared blowback Hoogsteen exchange are shown in Fig. 5b and Supplementary Figure S9b.

Prior studies (Kimsey et al. 2018) have shown that at high pH > ~8.0, G·T mismatches can dynamically exchange with tautomeric and anionic states in a star-like or a triangular (Trott and Palmer 2004) exchange topology. The exchange topology for the exchange of the G·T mismatch in s1GT-GGC at pH 8.8 and 10 °C was determined by fitting of the <sup>15</sup>N *R*<sub>1ρ</sub> data for G15-N1 and T5-N3. Based on the Akaike (Wagenmakers and Farrel 2004) and Bayesian (Burnham and Anderson 2004) information criterion weights, a statistically better fit was obtained for a triangular topology, with populations of the tautomeric and anionic state equal to 0.075 ± 0.005% and 8.019 ± 1.007%, respectively. The pKa ~9.9 for the ionization of the G·T mismatch thus obtained was inconsistent with prior estimations (Kimsey et al. 2018) of the pKa ~11 made based on <sup>15</sup>N *R*<sub>1ρ</sub> data for the G·T mismatch in s1GT-GGC at 10 °C at pH values of 8.0 and 8.4, respectively. Thus, the <sup>15</sup>N and <sup>13</sup>C *R*<sub>1ρ</sub> profiles for G15-N1, T5-N3 and T5-C4' in s1GT-GGC at pH 8.8 and 10 °C were fit assuming 3-state exchange between wobble, tautomeric and anionic G·T mismatches in a star-like (Trott and Palmer 2004) exchange topology (Supplementary Figure S11a) instead to yield exchange parameters in Supplementary Table S7. The large error in the fitted  $\Delta\omega_{T5-C4'}$  for the tautomeric G·T excited state (Supplementary Table S7) is due its low population (0.065 ± 0.003%) and fast exchange rate (4029 ± 352 s<sup>-1</sup>), which results in a small contribution to the observed RD profile, thereby making determination of  $\Delta\omega$  unreliable.

The uncertainties in the exchange parameters were computed using a Monte-Carlo scheme (Bothe et al. 2014). Alignment of magnetization during B-M fitting

was performed as described previously (Rangadurai et al. 2019). Off-resonance *R*<sub>1ρ</sub> profiles were generated by plotting  $(R_2 + R_{ex}) = (R_{1\rho} - R_1 \cos^2 \theta) / \sin^2 \theta$ , where  $\theta$  is the angle between the effective field of the observed resonance and the z-axis, as a function of  $\Omega = \omega_{OBS} - \omega_{RF}$ , where  $\omega_{OBS}$  is the Larmor frequency of the observed resonance and  $\omega_{RF}$  is the angular frequency of the applied spin-lock.

## Results and discussion

### Wobble G·T mismatches have a distinct sugar-backbone conformation relative to canonical Watson–Crick base pairs

Before examining whether transitions between wobble and WC-like G·T mismatches entail changes in the sugar-backbone conformation, we first examined how and why the sugar-backbone conformation differs for wobble G·T relative to canonical WC G·C or A·T bps. If we were to start with a canonical WC G·C bp, the introduction of a G·T mismatch by replacing the C with a T would result in steric clashes between the imino hydrogen atoms. The steric clashes can be resolved through translation of the two bases by one hydrogen bond register to form a paired wobble G·T mismatch in which the T is displaced toward the major groove relative to the G. It is this movement of the bases to accommodate the wobble pair that will require changes in the sugar-backbone conformation (Allawi et al. 1998; Patel et al. 1982; Hare et al. 1986; Hunter et al. 1987).

To capture the changes in the sugar-backbone conformation required to accommodate the G·T wobble, we surveyed (“Materials and methods” section) existing crystal structures of DNA duplexes containing G·T mismatches. We find that relative to WC G·C and A·T bps, wobble G·T mismatches have sugar puckers that are biased away from C2'-endo towards puckers in between C2' and C3'-endo, and backbone torsion angles  $\xi$  and  $\zeta$  that are biased away from the BII conformation for both G and T nucleotides (Fig. 2a, Supplementary Figure S1). While it is often assumed that the T (or U) base primarily moves to form a wobble (Westhof et al. 2019; Westhof 2014), the structures show both bases move to form the wobble pair as noted previously for G·T mismatches in A-DNA (Rabinovich et al. 1988) (Fig. 2b).

To further evaluate the robustness of the above results, we carried out 0.5  $\mu$ s long MD simulations using the parmbsc0 forcefield (Cheatham et al. 1999; Perez et al. 2007) on DNA duplexes containing either G·T, G·C, or A·T bps (see “Materials and methods” section). In agreement with the crystal structure survey, the simulations show changes in the backbone torsion angles  $\xi$  and  $\zeta$  away from the BII conformation at the G of the G·T mismatch, in addition to a bias away from the C2'-endo sugar pucker towards puckers

in between C2' and C3'-endo, at both the G and T of the G·T mismatch (Fig. 3, Supplementary Figure S3).

### Sugar carbon chemical shifts for wobble G·T mismatches differ from canonical Watson–Crick base pairs

The differences in the sugar-backbone conformation, particularly the sugar pucker, between wobble G·T and canonical WC bps (Figs. 2 and 3) are expected to give rise to differences in sugar carbon chemical shifts. The C3' chemical shift is highly sensitive to sugar pucker while C4' is sensitive to both sugar pucker and the backbone angle  $\gamma$  (Santos et al. 1989; Fonville et al. 2012; Dejaegere and Case 1998; Xu and Au-Yeung 2000). If these changes in chemical shifts were sizeable (i.e. > 1 ppm), NMR RD measurements targeting sugar C3'/C4' nuclei of the G·T mismatch could be used to examine whether transitions toward low-abundance short-lived WC-like conformations restore C3'/C4' chemical shifts and sugar-backbone geometry typical of the canonical WC conformation. It should be noted that based on prior studies (Kimsey et al. 2015) it is not possible to infer the sugar-backbone geometry of WC-like G·T mismatches using the C1' carbons as probes as they are not sensitive to the wobble to WC-like transition.

For two different DNA sequence contexts, we compared the sugar C3' and C4' chemical shifts of the wobble G·T mismatch with those of G·C and A·T WC bps. We used

DNA duplexes containing either G·C or A·T bps in place of G·T (Fig. 1c, Supplementary Figure S4). Indeed, relative to either G·C or A·T bps, wobble G·T mismatches consistently have upfield shifted ( $\sim 1$ –3 ppm) sugar chemical shifts which are particularly sizeable for G·C3', T·C3', and T·C4' (Fig. 4, Supplementary Figure S5). Such upfield shifted sugar chemical shifts observed for G·T mismatches are exactly as expected for a bias away from a C2'-endo conformation, in agreement with the structure survey (Fig. 2), MD simulations (Fig. 3), prior chemical shift measurements (Shi et al. 2018; Rangadurai et al. 2018; Santos et al. 1989) and Density Functional Theory (DFT) calculations (Fonville et al. 2012; Dejaegere and Case 1998). Additional measurements of  $^{31}\text{P}$  chemical shifts and  $J_{\text{H}3'-\text{P}}$  coupling constants (Gorenstein 1994) are required for characterizing mismatch induced changes in BI/BII phosphate conformations.

Furthermore, the observation of chemical shift perturbations for both the T and G (Fig. 4c) indicates that both residues experience a change in the sugar-backbone on formation of a wobble bp, as expected based on the comparison of crystal structures (Fig. 2b) (Rabinovich et al. 1988). The G·T wobble also induces sizeable chemical shift perturbations in the neighboring WC bps that are particularly large for the 3' neighbor of the T and the 5' neighbor of the G (Fig. 4b). These perturbations likely reflect additional potentially destabilizing conformational changes in neighboring bps that help to accommodate the movement of the T and G to form a wobble bp.

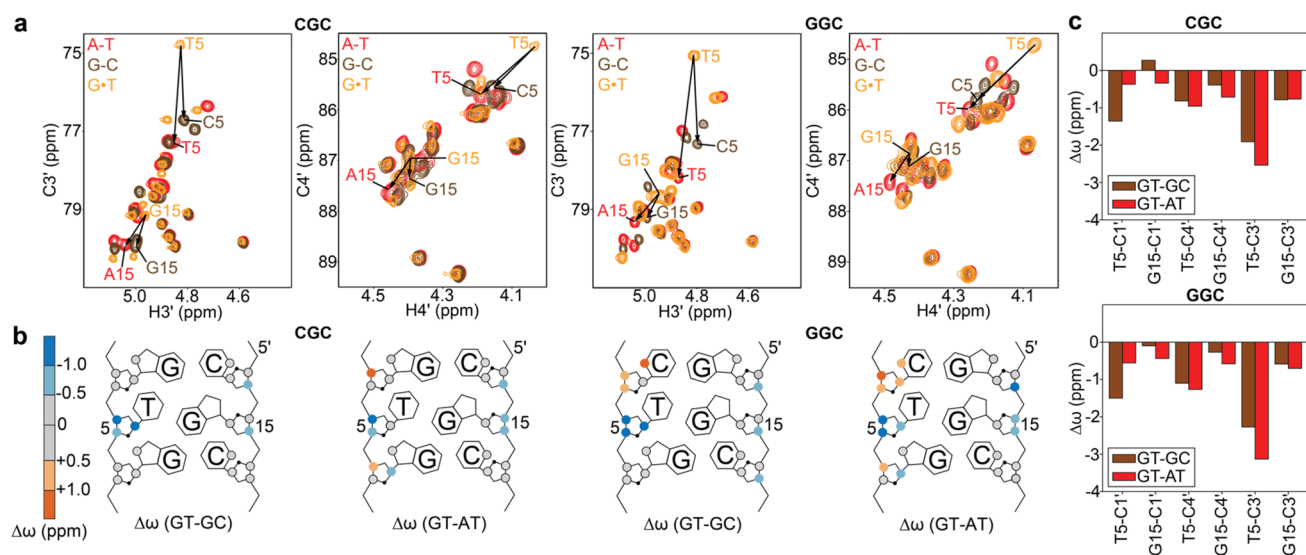
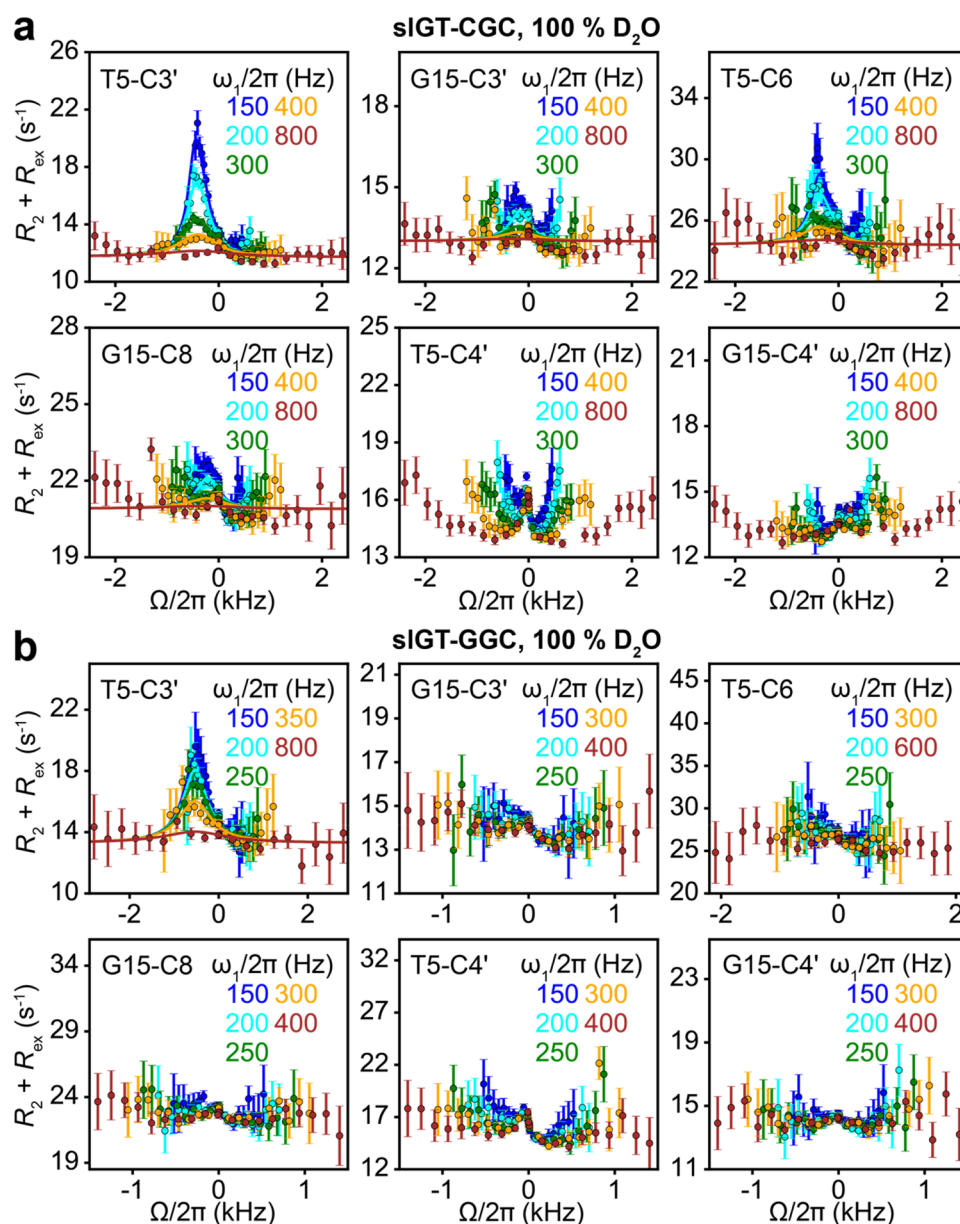


**Fig. 4** **a** Chemical shift overlays of the C3'-H3' and C4'-H4' regions of 2D  $^{13}\text{C}$ ,  $^1\text{H}$  HSQC spectra for GT-CGC/GT-GGC (yellow), GC-CGC/GC-GGC (brown) and AT-CAC/AT-GAC (red). **b** Chemical shift perturbations induced by the G·T mismatch relative to G·C (GT-GC) or A·T (GT-AT) bps. **c** Bar plot of the  $\Delta\omega$  for the sugar carbons of the G·T mismatch containing hairpins relative to those containing G·C (brown) or A·T (red) bps

**Fig. 5**  $^{13}\text{C}$  off-resonance  $R_{1\rho}$  RD profiles measured for **a** sIGT-CGC and **b** sIGT-GGC hairpins at pH 6.9 and 25 °C in 100%  $\text{D}_2\text{O}$ . Shown are experimental data points with a global fit to the Bloch–McConnell equations (solid lines) assuming a 3-state exchange process in a star-like (Trott and Palmer 2004) topology with shared exchange parameters for the wobble to WC-like exchange of the G·T mismatch and the Hoogsteen blowback exchange contribution for sIGT-CGC, and a fit to a 2-state exchange model for sIGT-GGC (Materials and Methods). Error bars represent the experimental uncertainty of the  $R_{1\rho}$  data and were computed as described previously by propagating the experimental error in  $R_{1\rho}$  (Rangadurai et al. 2019). Spin-lock powers are color-coded

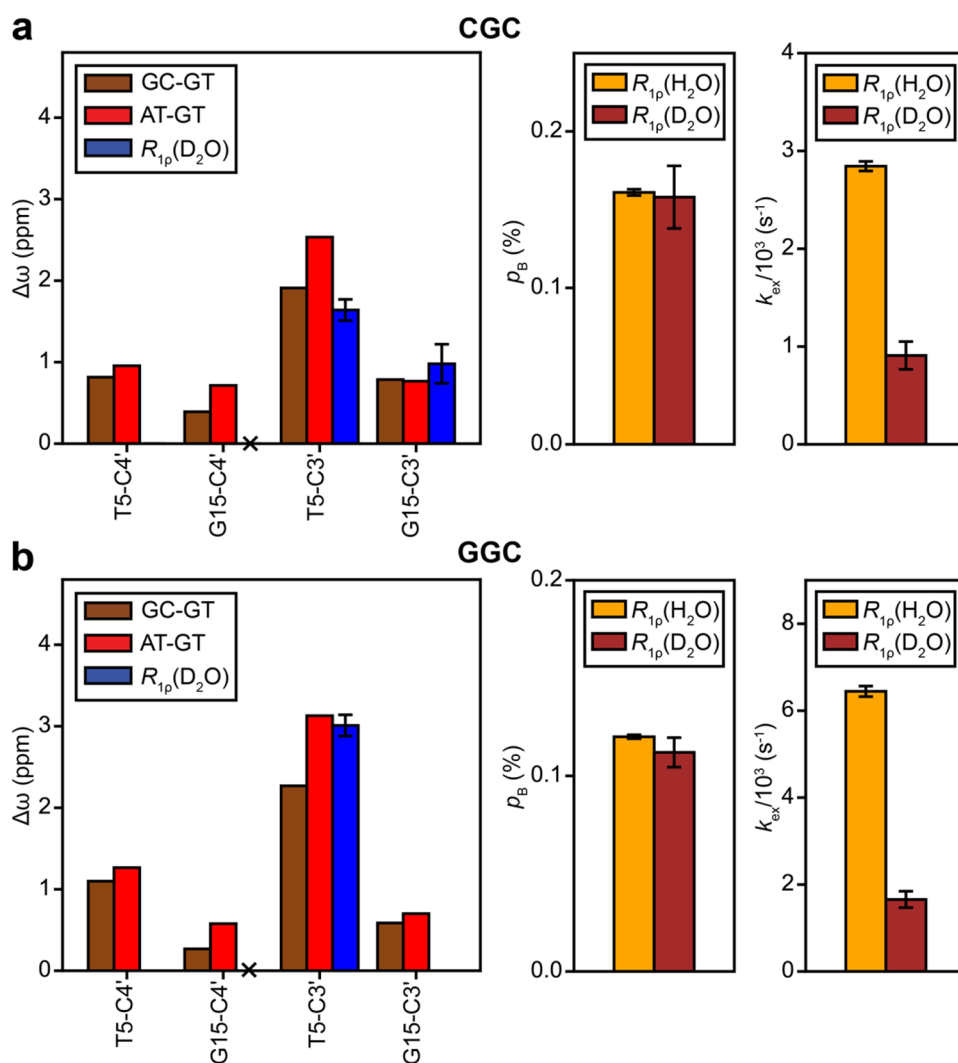


### Tautomeric Watson–Crick-like G·T mismatches have sugar chemical shifts that are similar to Watson–Crick base pairs

Based on the above results, transitions between wobble and WC-like G·T mismatches are predicted to lead to large changes ( $> 1$  ppm) in the G-C3', T-C3' and T-C4' chemical shifts if they entail changes in the sugar-backbone to a WC-like conformation. These chemical shift perturbations are large enough to give rise to detectable NMR  $R_{1\rho}$  RD. In contrast, we do not expect sizeable RD for G-C4' because the changes in chemical shifts are predicted to fall near or below the RD detection limit ( $< 1$  ppm).

We tested the above predictions by measuring off-resonance  $R_{1\rho}$  RD profiles for G15-C3', G15-C4', T5-C3' and T5-C4' in the sIGT-CGC and sIGT-GGC DNA hairpins (Fig. 5, Supplementary Tables S4 and S6, “Materials and methods” section) at pH 6.9 and  $T = 25$  °C in  $\text{D}_2\text{O}$ . Under these pH conditions, any contribution to the RD profiles from the transient formation of the anionic G·T<sup>-</sup> mismatch ( $p_B \sim 0.001\%$ ) can be safely ignored. Thus, RD profiles are expected to sense the two state exchange between wobble and tautomeric WC-like G·T mismatches. Experiments were performed in  $\text{D}_2\text{O}$  to minimize interference from the water signal (“Materials and methods” section). To allow comparison with prior results (Szymanski et al. 2017; Kimsey et al.

**Fig. 6** Comparison of  $\Delta\omega$  of the sugar carbons for the formation of a WC-like G-T mismatch, estimated as the difference in chemical shifts between hairpins containing G-C and G-T bps (brown), A-T and G-T bps (red) and those obtained from  $^{13}\text{C}$   $R_{1\rho}$  measurements in 100%  $\text{D}_2\text{O}$  (blue). Nuclei for which  $\Delta\omega < 0.5$  ppm are not expected to show detectable RD and are indicated using a 'X' symbol. Also shown are  $p_B$  and  $k_{\text{ex}}$  for the formation of WC-like G-T mismatches obtained using  $^{13}\text{C}$  and  $^{15}\text{N}$   $R_{1\rho}$  measurements in 90%  $\text{H}_2\text{O}$ :10%  $\text{D}_2\text{O}$  (yellow) and  $^{13}\text{C}$   $R_{1\rho}$  measurements in 100%  $\text{D}_2\text{O}$  (brown). The data is shown for sequence contexts CGC (a) and GGC (b). Error bars denote uncertainty in the fitted parameters determined using a Monte-Carlo scheme (Bothe et al. 2014) when fitting the  $R_{1\rho}$  data for slGT-CGC to a 3-state exchange model with shared exchange parameters, and the data for slGT-GGC to a 2-state exchange model, as described in the Materials and Methods



2018; Kimsey et al. 2015), we also measured  $^{15}\text{N}$  and  $^{13}\text{C}$   $R_{1\rho}$  RD profiles for G-N1, T-N3, G-C8 and T-C6 in water (Supplementary Figure S9, Supplementary Tables S3 and S5), as well as for G-C8 and T-C6 carbons, which are known probes for the wobble to WC-like transition, in  $\text{D}_2\text{O}$  (Fig. 5, Supplementary Table S4).

As predicted, sizeable off-resonance  $R_{1\rho}$  RD profiles were observed for G15-C3' and T5-C3' in slGT-CGC, and T5-C3' in slGT-GGC whereas the profiles were weaker and in most cases undetectable for T5-C4' and G15-C4' (Fig. 5). The lack of observed RD for G15-C3' in slGT-GGC is likely due to its small  $\Delta\omega$  ( $\sim 1$  ppm) coupled with its faster rate of exchange ( $1657 \pm 189 \text{ s}^{-1}$ ) to form a WC-like species relative to slGT-CGC ( $909 \pm 142 \text{ s}^{-1}$ , Supplementary Tables S4 and S6). The lack of observable RD for T5-C4' in both slGT-CGC and slGT-GGC is likely because of the small  $\Delta\omega$  ( $\sim 1$  ppm, see Fig. 4c).

The C3' RD profiles could be fit satisfactorily to exchange models involving a dominant ground state (GS)

and a sparsely populated excited state (ES) (Mulder et al. 2001) (Fig. 5, Supplementary Figs. S6–S8, “Materials and methods” section). The fits yielded exchange parameters of interest, including the ES population ( $p_{\text{ES}}$ ), the GS $\leftrightarrow$ ES exchange rate ( $k_{\text{ex}} = k_1 + k_{-1}$ , where  $k_1$  and  $k_{-1}$  are the forward and backward rate constants), and the chemical shift difference between the ES and GS ( $\Delta\omega = \omega_{\text{ES}} - \omega_{\text{GS}}$ ), which carries structural information.

The  $\Delta\omega$  values deduced from fitting the sugar C3' RD data were in excellent agreement with those expected for a transition between the wobble and WC-like conformation, estimated as the difference between the chemical shifts of WC G-C/A-T bps and wobble G-T mismatches (Fig. 6). In addition, the ES populations were in very good agreement with values obtained independently from fitting base G-C8 and T-C6, and imino nitrogen G-N1 and T-N3 RD data in  $\text{H}_2\text{O}$  (Kimsey et al. 2018; Kimsey et al. 2015) (Fig. 6, Supplementary Figure S8a, Supplementary Tables S3–S6).

However, the  $k_{\text{ex}}$  measured in  $\text{D}_2\text{O}$  was  $\sim 3.5$  fold slower than values measured in  $\text{H}_2\text{O}$ .

Based on DFT studies (Nomura et al. 2013; Brovarets 2015), the transition state for conversion between wobble and tautomeric WC-like G-T entails movement of a proton from G-O6 to T-O4 (Supplementary Figure S10). If this were the case, we would expect a  $\sim 2$ -4 fold reduction in the rate of the reaction in  $\text{D}_2\text{O}$  versus  $\text{H}_2\text{O}$  (Anslyn 2005). Such isotope effects have previously been reported in studies of conformational changes involving proton transfer in proteins (Watt et al. 2007). The reduced  $k_{\text{ex}}$  in  $\text{D}_2\text{O}$  versus  $\text{H}_2\text{O}$  therefore provides the first experimental evidence in support of a transition state for tautomerization involving proton transfer. While additional experiments including measurement of RD as a function of viscosity are needed to rule out that the observed change in  $k_{\text{ex}}$  is not due to a change in viscosity between  $\text{D}_2\text{O}$  and  $\text{H}_2\text{O}$  (Watt et al. 2007), this highlights the general utility of kinetic isotope effects in the RD-based characterization of nucleic acid transition states. Taken together, the sugar RD data shows that the sugar-backbone adopts a WC-like conformation when forming the tautomeric WC-like G-T mismatch.

### Probing the sugar conformation of anionic G-T<sup>-</sup> base pair

We also used sugar RD to probe the sugar-backbone conformation of the anionic G-T<sup>-</sup> ES observed at high pH (Kimsey et al. 2018; Kimsey et al. 2015). Ionization of T at high

pH ( $> 8.0$ ) was previously inferred based on the appearance of a second pH dependent ES with a large ( $\sim 50$  ppm) downfield shift in T-N3 (Kimsey et al. 2018; Kimsey et al. 2015). However, in addition to a WC-like conformation, a G-T<sup>-</sup> mismatch can also form an ‘inverted wobble’ conformation in which the bases move by one additional hydrogen bond register past WC pairing (Fig. 7a). Inverted G-T wobble bps have previously been observed crystallographically (Johnson and Beese 2004; Xia and Konigsberg 2014) and more recently, G-U inverted wobbles have been observed in the context of modified bases at the wobble position of the tRNA-mRNA mini-helix in the ribosome (Rozov et al. 2016). The inverted wobble was not suggested to contribute significantly to the anionic G-T<sup>-</sup> ES based on DFT calculations in a prior study (Kimsey et al. 2015). The measured  $\Delta\omega$  (56 ppm) of T-N3 for the anionic ES was in good agreement with DFT calculations assuming a Watson-Crick like ES ( $\Delta\omega = 54$  ppm), and was different from the calculated  $\Delta\omega$  for an inverted wobble ( $\Delta\omega = 46$  ppm). However, direct experimental data is needed to rule out the possibility that the ES observed at high pH is a WC-like conformation not an inverted wobble.

Given the greater movement of the bases in forming an inverted wobble relative to WC, we hypothesized that the inverted wobble has a unique sugar-backbone conformation, and in turn, unique sugar chemical shifts distinct from those of canonical WC bps. If this were the case, sugar RD data could be used to rule out an inverted anionic wobble G-T<sup>-</sup> ES. We used G to isoguanosine (isoG) substitution

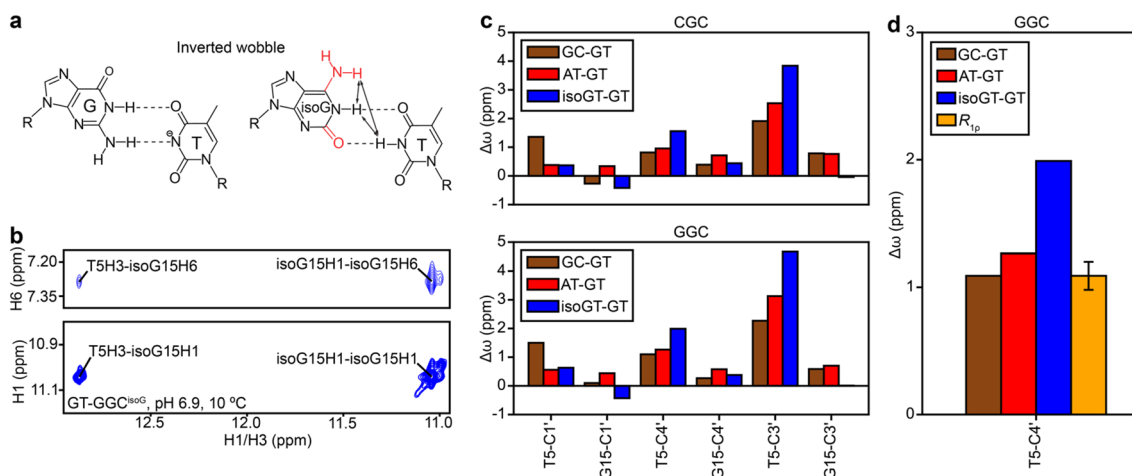


**Fig. 7** **a** Chemical structures of G-T<sup>-</sup> and isoG-T inverted wobble bps. Chemically modified sites in isoG are indicated in red. Arrows on the isoG-T bp denote characteristic NOE connectivities expected for the inverted wobble. **b** 2D  $^1\text{H}$ ,  $^1\text{H}$  NOESY spectrum of the imino-imino and imino-amino region for GT-GGC<sup>isoG</sup>. **c** Comparison of  $\Delta\omega$  of the sugar carbons for the formation of a WC-like G-T mismatch, estimated as the difference in chemical shift between hairpins containing G-C and G-T bps (brown) or A-T and G-T bps (red). Also shown is the  $\Delta\omega$  for the formation of an inverted wobble G-T<sup>-</sup> mismatch, esti-

ated as the difference in chemical shift between hairpins containing isoG-T and G-T bps (blue). **d** Comparison of  $\Delta\omega$  for T5-C4' for the formation of a WC-like (brown and red) or inverted wobble G-T mismatch (blue), with the experimental value for the G-T<sup>-</sup> ES obtained from  $R_{1\rho}$  measurements (yellow) on GT-GGC at pH 8.8 and 10 °C in 90%  $\text{H}_2\text{O}$ :10%  $\text{D}_2\text{O}$  (Materials and Methods). The uncertainty in  $\Delta\omega$  denotes the fitting error estimated using a Monte-Carlo scheme as described previously (Bothe et al. 2014)

(Robinson et al. 1998) to stabilize an inverted wobble conformation (Fig. 7a) and thereby deduce its sugar chemical shifts. While the chemical modification of the G and lack of ionization of the T would not be expected to faithfully reproduce the base chemical shifts of the inverted wobble G·T<sup>-</sup>, the sugar chemical shifts should not be significantly affected by chemical modification of the base (Xu and Au-Yeung 2000).

2D [<sup>1</sup>H, <sup>1</sup>H] NOESY spectra showed cross peaks between T-H3, isoG-H1 and isoG-H6 as expected for an inverted wobble isoG·T bp (Fig. 7b). Furthermore, 2D HSQC spectra (Supplementary Figure S5) revealed that the T-C3' and the T-C4' sugar carbon chemical shifts are more downfield shifted for the inverted wobble relative to the WC conformation. Therefore, transition of a wobble G·T to an inverted wobble G·T<sup>-</sup> is expected to result in a larger downfield chemical shift for T-C3' and T-C4' relative to a transition toward the WC-like G·T<sup>-</sup> conformation (Fig. 7c). In contrast, the other sugar carbon chemical shifts (T-C1', G-C1', G-C3', G-C4') were small (< 1 ppm) and/or similar to the shifts expected for a WC bp (Fig. 7c), and therefore were less suited for distinguishing inverted wobble versus WC-like G·T<sup>-</sup> conformations using RD.

We therefore chose T-C3' and T-C4' as RD probes as they should in theory be able to distinguish between the inverted wobble and WC-like G·T<sup>-</sup> conformation. In principle, one can obtain these sugar chemical shifts for G·T<sup>-</sup> by fitting the sugar RD data measured at high pH. However, in practice, owing to the small magnitude of the exchange contributions in the RD profiles, fitting the sugar RD data to a 3-state exchange process involving the wobble, tautomeric and anionic species yields unreliable estimates for the exchange parameters, including the chemical shifts. The exchange parameters can be more reliably determined with the inclusion of RD data from G-N1 and T-N3 RD owing to their much larger exchange contributions in the RD profiles, which is a consequence of the large changes in chemical shifts during tautomerization and ionization (Kimsey et al. 2018). This in turn necessitates that the RD be measured in H<sub>2</sub>O. While this complicates C3' RD measurements owing to the fact that the H3' protons are close to the water resonance frequency, this is not an issue for the C4' RD measurements as the H4' protons are relatively farther away from water. Thus, our strategy to rule out the inverted wobble conformation for the G·T<sup>-</sup> anionic ES involved performing imino nitrogen and T-C4' RD measurements in H<sub>2</sub>O.

The imino G15-N1 and T5-N3, and sugar T5-C4' RD profiles for sIGT-GGC could be globally fitted together to a 3-state exchange process between wobble, tautomeric and anionic ES G·T bps in a star-like topology (Kimsey et al. 2018; Trott and Palmer 2004) (Supplementary Figure S11a, “Materials and methods” section) to obtain exchange parameters (Supplementary Table S7). The difference in chemical

shifts between the GS and anionic ES for T-C4' was found to be in better agreement with that expected for formation of a WC-like bp as compared to an inverted wobble (Fig. 7d). Moreover, the quality of the fit worsened when fixing the  $\Delta\omega$  to be equal to the value expected for an inverted wobble G·T<sup>-</sup> bp (Supplementary Figure S11b). These data indicate that the anionic G·T<sup>-</sup> ES has a WC-like conformation and help to rule out the alternative inverted wobble conformation.

## Discussion

Determining the structures of short-lived low-abundance excited conformational states of biomolecules, such as the WC-like G·T mismatches studied in this work presents a significant challenge to conventional biophysical methods. NMR RD experiments provide a rare opportunity to detect such ESs as well as to probe their conformations (Rangadurai et al. 2019; Sekhar and Kay 2013; Korzhnev and Kay 2008; Hansen et al. 2008; Xue et al. 2015; Zhao and Zhang 2015). In both proteins and nucleic acids, measurements of RD data for a variety of spins is crucial for accurately deducing the ES conformation (Shi et al. 2018; Sathyamoorthy et al. 2017; Hansen et al. 2008). Prior studies (Shi et al. 2018; Clay et al. 2017) have highlighted the utility of sugar RD data in characterizing ES Hoogsteen bps in DNA and ESs involving alternative secondary structures in RNA. In this study, the sugar RD data could be used to obtain new evidence in support of an ES that involves tautomeric and anionic WC-like G·T conformations. It should be noted that the lack of detectable RD on the C1' carbons of the G·T mismatch, in spite of the known sensitivity of the C1' chemical shift to changes in sugar pucker (Santos et al. 1989; Fonville et al. 2012; Dejaegere and Case 1998; Xu and Au-Yeung 2000) that accompany formation of a WC-like mismatch (Figs. 2 and 3) is likely due to compensatory changes in  $\chi$  angle (Supplementary Figs. 1 and 3). Such compensation effects the  $\chi$ -angle and sugar pucker have previously been noted in the context of RNA (Zhou et al. 2016) and DNA (Shi et al. 2018).

While it is not surprising that tautomeric WC-like G·T mismatches adopt a WC-like sugar-backbone conformation, the results help to rule out an inverted wobble conformation for the case of anionic G·T<sup>-</sup> mismatches. The WC-like sugar-backbone conformation further supports a mutagenic role for these fleeting WC-like states as this is likely to align functional groups for phosphodiester bond formation during catalysis by DNA polymerases. Based on these results, it is very likely that base modifications that stabilize ionization and promote miscoding such as 5-Bromo and Fluoro uridine (Yu et al. 1993), and Uridine 5-oxyacetic acid (Strebiter et al. 2018) do so in part via formation of a WC-like ES conformation.

Our studies add to a growing view that in duplex DNA, non-canonical bps such as Hoogsteen and wobble G·T mismatches have sugar puckers that are biased away from the canonical C2'-endo conformation. In this regard, it is interesting to note that prior NMR studies indicated that the sugar pucker at wobble G·T mismatches is C2'-endo (Allawi and SantaLucia 1998; Hare et al. 1986) and not biased away from the C2'-endo conformation as inferred here based on analysis of chemical shifts and MD simulations. This discrepancy is likely due to the absence of *J*-coupling restraints for constraining the sugar pucker during structure refinement in the study by Hare et al. (Hare et al. 1986) and possibly due to differences in sequence context in the study by Allawi and SantaLucia (1998). It is also interesting to note that changes in backbone angles and movements of the bases required for the formation of wobble G·T mismatches identified in this study (Figs. 2 and 3) qualitatively mirror those recently described for non-canonical A·T Hoogsteen bps (Shi et al. 2018; Sathyamoorthy et al. 2017) in which the bases have to come into proximity without changes in the hydrogen bond register

Crystal structures of some DNA polymerases in complex with DNA, especially those belonging to the A-family, show that the WC base paired DNA near the incoming correct base pair bp typically adopts a conformation intermediate between A and B forms, with C3'-endo sugar puckers and a wide minor groove (Kiefer et al. 1998; Eom et al. 1996; Batra et al. 2006). Thus, further studies of G·T/G·U mismatches in analogous environments such as RNA–DNA hybrids or A-RNA could shed light into the nature of the sugar-backbone changes required for formation of WC-like G·T mismatches in these contexts, and consequently DNA conformational changes required for misincorporation by these DNA polymerases. Additional studies are also needed to characterize DNA sugar-backbone dynamics within the physiologically relevant polymerase active site environment. The sugar RD data can also be measured in flexible environments mimicking physiological substrates of DNA polymerases such as mismatches at the terminal ends, where <sup>15</sup>N base RD measurements may be compromised due to exchange of the imino protons with solvent. More generally, the approach outlined in this study can also be extended to other mismatches to probe their mutagenic conformations, especially given the difficulties with observing imino signals in mismatches such as A·C (Gao and Patel 1987; Patel et al. 1984).

**Acknowledgements** We would like to thank Dr. Eric Westhof for helpful discussions pertaining to the inverted wobble and members of the Al-Hashimi lab for their critical input.

**Funding** This work was supported by the US National Institutes of Health (R01GM089846) and US National Institutes

of General Medical Sciences (P01GM0066275) Grants to H. M. A.

## Compliance with ethical standards

**Conflict of interest** The authors declare that they have no conflict of interest.

**Open Access** This article is licensed under a Creative Commons Attribution 4.0 International License, which permits use, sharing, adaptation, distribution and reproduction in any medium or format, as long as you give appropriate credit to the original author(s) and the source, provide a link to the Creative Commons licence, and indicate if changes were made. The images or other third party material in this article are included in the article's Creative Commons licence, unless indicated otherwise in a credit line to the material. If material is not included in the article's Creative Commons licence and your intended use is not permitted by statutory regulation or exceeds the permitted use, you will need to obtain permission directly from the copyright holder. To view a copy of this licence, visit <http://creativecommons.org/licenses/by/4.0/>.

## References

- Allawi HT, SantaLucia J Jr (1998) NMR solution structure of a DNA dodecamer containing single G·T mismatches. *Nucleic Acids Res* 26:4925–4934
- Anslyn EV, Dougherty DA (2005) *Modern physical organic chemistry*. Univeristy Science Books, Sausalito
- Batra VK et al (2006) Magnesium-induced assembly of a complete DNA polymerase catalytic complex. *Structure* 14:757–766
- Bebenek K, Pedersen LC, Kunkel TA (2011) Replication infidelity via a mismatch with Watson-Crick geometry. *Proc Natl Acad Sci USA* 108:1862–1867
- Berendsen HJC, Grigera JR, Straatsma TP (1987) The missing term in effective pair potentials. *J Phys Chem* 91:6269–6271
- Berman HM et al (2000) The protein data bank. *Nucleic Acids Res* 28:235–242
- Bothe JR, Stein ZW, Al-Hashimi HM (2014) Evaluating the uncertainty in exchange parameters determined from off-resonance R1rho relaxation dispersion for systems in fast exchange. *J Magn Reson* 244:18–29
- Brovarets OO, Hovorun DM (2015) How many tautomerization pathways connect Watson-Crick-like G\*·T DNA base mispair and wobble mismatches? *J Biomol Struct Dyn* 33:2297–2315
- Budowsky EI (1976) The mechanism of the mutagenic action of hydroxylamines. *Prog Nucleic Acid Res Mol Biol* 16:125–188
- Burnham KP, Anderson DR (2004) Multimodel inference: understanding AIC and BIC in model selection. *Soc. Meth. Res.* 33:261–304
- Cantara WA, Murphy FVT, Demirci H, Agris PF (2013) Expanded use of sense codons is regulated by modified cytidines in tRNA. *Proc Natl Acad Sci USA* 110:10964–10969
- Cheatham TE 3rd, Cieplak P, Kollman PA (1999) A modified version of the Cornell et al. force field with improved sugar pucker phases and helical repeat. *J Biomol Struct Dyn* 16:845–862
- Clay MC, Ganser LR, Merriman DK, Al-Hashimi HM (2017) Resolving sugar puckers in RNA excited states exposes slow modes of repuckering dynamics. *Nucleic Acids Res* 45:e134
- Dejaegere AP, Case DA (1998) Density functional study of ribose and deoxyribose chemical shifts. *J Phys Chem A* 102:5280–5289

- Delaglio F et al (1995) NMRPipe: a multidimensional spectral processing system based on UNIX pipes. *J Biomol NMR* 6:277–293
- Demeshkina N, Jenner L, Westhof E, Yusupov M, Yusupova G (2012) A new understanding of the decoding principle on the ribosome. *Nature* 484:256–259
- Eom SH, Wang J, Steitz TA (1996) Structure of Taq polymerase with DNA at the polymerase active site. *Nature* 382:278–281
- Fonville JM et al (2012) Chemical shifts in nucleic acids studied by density functional theory calculations and comparison with experiment. *Chemistry* 18:12372–12387
- Freudenthal BD, Beard WA, Cuneo MJ, Dyrkheeva NS, Wilson SH (2015) Capturing snapshots of APE1 processing DNA damage. *Nat Struct Mol Biol* 22:924–931
- Gao XL, Patel DJ (1987) NMR studies of A.C mismatches in DNA dodecanucleotides at acidic pH. Wobble A(anti).C(anti) pair formation. *J Biol Chem*. 262:16973–16984
- Gorenstein DG (1994) Conformation and dynamics of DNA and protein-DNA complexes by 31P NMR. *Chem Rev* 94:1315–1338
- Hansen DF, Vallurupalli P, Kay LE (2008a) Using relaxation dispersion NMR spectroscopy to determine structures of excited, invisible protein states. *J Biomol NMR* 41:113–120
- Hansen DF, Vallurupalli P, Lundstrom P, Neudecker P, Kay LE (2008b) Probing chemical shifts of invisible states of proteins with relaxation dispersion NMR spectroscopy: how well can we do? *J Am Chem Soc* 130:2667–2675
- Hansen AL, Nikolova EN, Casiano-Negroni A, Al-Hashimi HM (2009) Extending the range of microsecond-to-millisecond chemical exchange detected in labeled and unlabeled nucleic acids by selective carbon R(1rho) NMR spectroscopy. *J Am Chem Soc* 131:3818–3819
- Hare D, Shapiro L, Patel DJ (1986) Wobble dG X dT pairing in right-handed DNA: solution conformation of the d(C-G-T-G-A-A-T-T-C-G-C-G) duplex deduced from distance geometry analysis of nuclear Overhauser effect spectra. *Biochemistry* 25:7445–7456
- Harris VH et al (2003) The effect of tautomeric constant on the specificity of nucleotide incorporation during DNA replication: support for the rare tautomer hypothesis of substitution mutagenesis. *J Mol Biol* 326:1389–1401
- Hunter WN et al (1987) The structure of guanosine-thymidine mismatches in B-DNA at 2.5-A resolution. *J Biol Chem* 262:9962–9970
- Ikeuchi Y et al (2010) Agmatine-conjugated cytidine in a tRNA anticodon is essential for AUA decoding in archaea. *Nat Chem Biol* 6:277–282
- Johnson SJ, Beese LS (2004) Structures of mismatch replication errors observed in a DNA polymerase. *Cell* 116:803–816
- Joung IS, Cheatham TE 3rd (2008) Determination of alkali and halide monovalent ion parameters for use in explicitly solvated biomolecular simulations. *J Phys Chem B* 112:9020–9041
- Kiefer JR, Mao C, Braman JC, Beese LS (1998) Visualizing DNA replication in a catalytically active *Bacillus* DNA polymerase crystal. *Nature* 391:304–307
- Kimsey IJ, Petzold K, Sathyamoorthy B, Stein ZW, Al-Hashimi HM (2015) Visualizing transient Watson-Crick-like mispairs in DNA and RNA duplexes. *Nature* 519:315–320
- Kimsey IJ et al (2018) Dynamic basis for dG\*dT misincorporation via tautomerization and ionization. *Nature* 554:195–201
- Koag MC, Lee S (2018) Insights into the effect of minor groove interactions and metal cofactors on mutagenic replication by human DNA polymerase beta. *Biochem J* 475:571–585
- Koag MC, Nam K, Lee S (2014) The spontaneous replication error and the mismatch discrimination mechanisms of human DNA polymerase beta. *Nucleic Acids Res* 42:11233–11245
- Korzhnev DM, Kay LE (2008) Probing invisible, low-populated States of protein molecules by relaxation dispersion NMR spectroscopy: an application to protein folding. *Acc Chem Res* 41:442–451
- Korzhnev DM, Orekhov VY, Kay LE (2005) Off-resonance R(1rho) NMR studies of exchange dynamics in proteins with low spin-lock fields: an application to a Fyn SH3 domain. *J Am Chem Soc* 127:713–721
- Kurata S et al (2008) Modified uridines with C5-methylene substituents at the first position of the tRNA anticodon stabilize U.G wobble pairing during decoding. *J Biol Chem* 283:18801–18811
- Lawley PD, Brookes P (1961) Acidic dissociation of 7:9-dialkylguanines and its possible relation to mutagenic properties of alkylating agents. *Nature* 192:1081–1082
- Lawley PD, Brookes P (1962) Ionization of DNA bases or base analogues as a possible explanation of mutagenesis, with special reference to 5-bromodeoxyuridine. *J Mol Biol* 4:216–219
- Li D et al (2014) Tautomerism provides a molecular explanation for the mutagenic properties of the anti-HIV nucleoside 5-aza-5,6-dihydro-2'-deoxycytidine. *Proc Natl Acad Sci USA* 111:E3252–E3259
- Lu XJ, Olson WK (2003) 3DNA: a software package for the analysis, rebuilding and visualization of three-dimensional nucleic acid structures. *Nucleic Acids Res* 31:5108–5121
- Lu XJ, Bussemaker HJ, Olson WK (2015) DSSR: an integrated software tool for dissecting the spatial structure of RNA. *Nucleic Acids Res* 43:e142
- Mulder FA, Mittermaier A, Hon B, Dahlquist FW, Kay LE (2001) Studying excited states of proteins by NMR spectroscopy. *Nat Struct Biol* 8:932–935
- Nikolova EN, Gottardo FL, Al-Hashimi HM (2012) Probing transient Hoogsteen hydrogen bonds in canonical duplex DNA using NMR relaxation dispersion and single-atom substitution. *J Am Chem Soc* 134:3667–3670
- Nomura K et al (2013) DFT calculations on the effect of solvation on the tautomeric reactions for Wobble Gua-Thy and Canonical Gua-Cyt base-pairs. *J Mod Phys* 4:422–431
- Palmer AG 3rd, Massi F (2006) Characterization of the dynamics of biomacromolecules using rotating-frame spin relaxation NMR spectroscopy. *Chem Rev* 106:1700–1719
- Patel DJ et al (1982) Structure, dynamics, and energetics of deoxyguanosine. Thymidine wobble base pair formation in the self-complementary d(CGTGAATTCGCG) duplex in solution. *Biochemistry* 21:437–444
- Patel DJ, Kozlowski SA, Ikuta S, Itakura K (1984) Deoxyadenosine-deoxycytidine pairing in the d(C-G-C-G-A-A-T-T-C-A-C-G) duplex: conformation and dynamics at and adjacent to the dA X dC mismatch site. *Biochemistry* 23:3218–3226
- Perez A et al (2007) Refinement of the AMBER force field for nucleic acids: improving the description of alpha/gamma conformers. *Biophys J* 92:3817–3829
- Phillips JH, Brown DM (1967) The mutagenic action of hydroxylamine. *Prog Nucl Acid Res Mol Biol* 7:349–368
- Rabinovich D, Haran T, Eisenstein M, Shakked Z (1988) Structures of the mismatched duplex d(GGGTGCCC) and one of its Watson-Crick analogues d(GGGCGCCC). *J Mol Biol* 200:151–161
- Rangadurai A et al (2018) Why are Hoogsteen base pairs energetically disfavored in A-RNA compared to B-DNA? *Nucleic Acids Res* 46:11099–11114
- Rangadurai A, Szymanski ES, Kimsey IJ, Shi H, Al-Hashimi HM (2019) Characterizing micro-to-millisecond chemical exchange in nucleic acids using off-resonance R1rho relaxation dispersion. *Prog Nucl Magn Reson Spectrosc* 112–113:55–102
- Robinson H et al (1998) 2'-Deoxyisoguanosine adopts more than one tautomer to form base pairs with thymidine observed by high-resolution crystal structure analysis. *Biochemistry* 37:10897–10905
- Roe DR, Cheatham TE 3rd (2013) PTRAJ and CPPTRAJ: software for processing and analysis of molecular dynamics trajectory data. *J Chem Theory Comput* 9:3084–3095

- Rozov A, Demeshkina N, Westhof E, Yusupov M, Yusupova G (2015) Structural insights into the translational infidelity mechanism. *Nat Commun* 6:7251
- Rozov A, Westhof E, Yusupov M, Yusupova G (2016a) The ribosome prohibits the G\*U wobble geometry at the first position of the codon-anticodon helix. *Nucleic Acids Res* 44:6434–6441
- Rozov A et al (2016b) Novel base-pairing interactions at the tRNA wobble position crucial for accurate reading of the genetic code. *Nat Commun* 7:10457
- Rozov A et al (2018) Tautomeric G\*U pairs within the molecular ribosomal grip and fidelity of decoding in bacteria. *Nucleic Acids Res* 46:7425–7435
- Salomon-Ferrer R, Gotz AW, Poole D, Le Grand S, Walker RC (2013) Routine microsecond molecular dynamics simulations with AMBER on GPUs: 2 explicit solvent particle mesh Ewald. *J Chem Theory Comput* 9:3878–3888
- Santos RA, Tang P, Harbison GS (1989) Determination of the DNA sugar pucker using  $^{13}\text{C}$  NMR spectroscopy. *Biochemistry* 28:9372–9378
- Sathyamoorthy B et al (2017) Insights into Watson-Crick/Hoogsteen breathing dynamics and damage repair from the solution structure and dynamic ensemble of DNA duplexes containing m1A. *Nucleic Acids Res* 45:5586–5601
- Sekhar A, Kay LE (2013) NMR paves the way for atomic level descriptions of sparsely populated, transiently formed biomolecular conformers. *Proc Natl Acad Sci USA* 110:12867–12874
- Sharma A, Kottur J, Narayanan N, Nair DT (2013) A strategically located serine residue is critical for the mutator activity of DNA polymerase IV from *Escherichia coli*. *Nucleic Acids Res* 41:5104–5114
- Shi H et al (2018) Atomic structures of excited state A-T Hoogsteen base pairs in duplex DNA by combining NMR relaxation dispersion, mutagenesis, and chemical shift calculations. *J Biomol NMR* 70:229–244
- Singer B, Spengler S (1981) Ambiguity and transcriptional errors as a result of modification of exocyclic amino groups of cytidine, guanosine, and adenosine. *Biochemistry* 20:1127–1132
- Sowers LC, Shaw BR, Veigl ML, Sedwick WD (1987) DNA base modification: ionized base pairs and mutagenesis. *Mutat Res* 177:201–218
- Strebitzer E et al (2018) 5-oxyacetic acid modification destabilizes double helical stem structures and favors anionic Watson-Crick like cmo(5) U-G base pairs. *Chemistry* 24:18903–18906
- Szymanski ES, Kimsey IJ, Al-Hashimi HM (2017) Direct NMR evidence that transient tautomeric and anionic states in dG.dT form Watson-Crick-like base pairs. *J Am Chem Soc* 139:4326–4329
- Topal MD, Fresco JR (1976a) Complementary base pairing and the origin of substitution mutations. *Nature* 263:285–289
- Topal MD, Fresco JR (1976b) Base pairing and fidelity in codon-anticodon interaction. *Nature* 263:289–293
- Trott O, Palmer AG 3rd (2004) Theoretical study of R(1rho) rotating-frame and R2 free-precession relaxation in the presence of n-site chemical exchange. *J Magn Reson* 170:104–112
- Vendeix FA et al (2012) Human tRNA(Lys3)(UUU) is pre-structured by natural modifications for cognate and wobble codon binding through keto-enol tautomerism. *J Mol Biol* 416:467–485
- Wagenmakers EJ, Farrell S (2004) AIC model selection using Akaike weights. *Psychon Bull Rev* 11:192–196
- Wang W, Hellinga HW, Beese LS (2011) Structural evidence for the rare tautomer hypothesis of spontaneous mutagenesis. *Proc Natl Acad Sci USA* 108:17644–17648
- Watson JD, Crick FH (1953) Genetical implications of the structure of deoxyribonucleic acid. *Nature* 171:964–967
- Watt ED, Shimada H, Kovrigin EL, Loria JP (2007) The mechanism of rate-limiting motions in enzyme function. *Proc Natl Acad Sci USA* 104:11981–11986
- Weixlbaumer A et al (2007) Mechanism for expanding the decoding capacity of transfer RNAs by modification of uridines. *Nat Struct Mol Biol* 14:498–502
- Westhof E (2014) Isostericity and tautomerism of base pairs in nucleic acids. *FEBS Lett* 588:2464–2469
- Westhof E, Yusupov M, Yusupova G (2019) The multiple flavors of GoU pairs in RNA. *J Mol Recognit* 32:e2782
- Woodside AM, Guengerich FP (2002) Effect of the O6 substituent on misincorporation kinetics catalyzed by DNA polymerases at O(6)-methylguanine and O(6)-benzylguanine. *Biochemistry* 41:1027–1038
- Xia S, Konigsberg WH (2014) Mispairs with Watson-Crick base-pair geometry observed in ternary complexes of an RB69 DNA polymerase variant. *Protein Sci* 23:508–513
- Xu X, Au-Yeung SCF (2000) Investigation of chemical shift and structure relationships in nucleic acids using NMR and density functional theory methods. *J Phys Chem B* 104:5641–5650
- Xue Y et al (2015) Characterizing RNA excited states using NMR relaxation dispersion. *Methods Enzymol* 558:39–73
- Goddard TD, Kneller DG (2008) SPARKY 3. San Francisco: University of California
- Yu H, Eritja R, Bloom LB, Goodman MF (1993) Ionization of bromouracil and fluorouracil stimulates base mispairing frequencies with guanine. *J Biol Chem* 268:15935–15943
- Zhao B, Zhang Q (2015) Characterizing excited conformational states of RNA by NMR spectroscopy. *Curr Opin Struct Biol* 30:134–146
- Zhou H et al (2016) m(1)A and m(1)G disrupt A-RNA structure through the intrinsic instability of Hoogsteen base pairs. *Nat Struct Mol Biol* 23:803–810
- Zimmer DP, Crothers DM (1995) NMR of enzymatically synthesized uniformly  $^{13}\text{C}/^{15}\text{N}$ -labeled DNA oligonucleotides. *Proc Natl Acad Sci USA* 92:3091–3095

**Publisher's Note** Springer Nature remains neutral with regard to jurisdictional claims in published maps and institutional affiliations.